Electrochimica Acta, 1968, Vol. 13, pp. 581 to 602. Pergamon Press. Printed in Northern Ireland

KINETICS OF THE HYDROGEN ELECTRODE REACTION ON GOLD IN ACID SULPHATE MELTS*

A. J. ARVIA, F. DE VEGA and H. A. VIDELA
Instituto Superior de Investigaciones, Facultad de Química y Farmacia,
Universidad Nacional de La Plata, La Plata, Argentina

Abstract—The hydrogen-electrode reaction on gold prepared in different ways has been investigated in molten acid sulphates at temperatures from *ca* 180 to 345°C. Potentiostatic and galvanostatic measurements under steady conditions were performed and the evolution of the potential of the working electrode when current was switched on and off was recorded.

Current/voltage curves followed a Tafel law at cathodic overvoltages higher than 0·050 V. Slopes ranging from $RT/2F$ to about $2RT/F$ are reported, depending on the preparation of the electrode, temperature and overvoltage region considered. Anodic current/voltage curves exhibit a limiting current. From the linear overvoltage/current region the reaction resistance was estimated for the anodic reaction. The exchange cds calculated from the reaction resistance agree with the values extrapolated from the Tafel lines having a slope $RT/2F$, if the stoichiometric number involved in the mechanism of the reaction is one.

Electrode potential decayed logarithmically with time. Experimental electrode capacitances were evaluated from the time dependence of electrode potential.

The hydrogen-electrode reaction is discussed in terms of a mechanism involving a fast hydrogen-ion discharge followed by a combination reaction as rate-determining step. The behaviour of the hydrogen-electrode reaction on gold in acid sulphate melts resembles that in aqueous acid solutions at ordinary temperatures.

Résumé—On a étudié la réaction du dégagement d'hydrogène sur des électrodes d'or preparées de diverses manières a des temperatures de 180 a 345°C dans des sulfates acides alcalins. Des mesures potentiostatiques et galvanostatiques dans des conditions stationnaires ont été obtenues et l'évolution du potentiel de l'électrode de travail pendant l'interruption ou la connection du courant a été enégistrée.

Les courbes de polarisation concordent avec l'équation de Tafel pour les surtensions cathodiques de plus 0,050 V. Des pentes comprises entre $RT/2F$ et $2RT/F$ furent obtenues, conditionées par la préparation de l'électrode et la région de surtension et température considérée. Les courbes de polarisation anodique montrent un courant limite. La résistance de la réaction de la région linéaire de la courbe de polarisation a été calculée pour la réaction anodique. Les courants d'échange obtenus de la résistance de la réaction concordent avec les valeurs extrapolées des lignes de Tafel avec une pente de $RT/2F$ quand le stoechismétrique est l'unité.

Le potentiel de l'électrode décroissait logarithmiquement avec les temps. Les capacités de l'électrode furent déduites de la dépendence du potentiel de l'électrode avec le temps.

On discute la réaction de l'électrode d'hydrogène sur la base d'un mécanisme comportant une décharge rapide de l'ion hydrogène suivie par une réaction de recombination comme étape régulatrice. Le comportement de la réaction de l'électrode d'hydrogène à sulfates alcalins acides fondus ressemble a celle des milieux aqueux a des temperatures ordinaires.

Zusammenfassung—Es wurde eine Untersuchung über die Kinetik der Reaktionen an der Wasserstoffelektrode in sauren Sulfatschmelzen an verschiedenartig hergestellten und vorbereiteten Goldelektroden bei Temperaturen zwischen 180 bis 345°C durchgeführt. Man verwendetè potentiostatische und galvanostatische zeitstationäre Methoden neben Messungen des zeitlichen Potentialverhaltens nach An- und Abschalten des Stromes. Für Überspannungen grösser als 0,050 V zeigen die Strom/Spannungskurven Tafelverhalten. Es wurden Tafelsteigungen zwischen RT/2F und ungefähr 2RT/F ermittelt, abhängig von der Herstellungsart der Elektroden, der Temperatur und dem überspannungsbereich. Die anodischen Strom/Spannungskurven zeigen ein Grenzstromgebiet. Aus dem linearen Bereich der Strom/Spannungskurve wurde für die Anodenreaktion der Reaktionswiderstand abgeschätzt. Die hieraus berechneten Austauschstromdichten stimmen mit den aus den Tafelgeraden mit der Steigung RT/2F extrapolierten Werten überein, falls man die stöchiometrische Zahl des Elektrodenvorganges zu eins annimmt. Die Abschaltkurven haben logarithmischen Charakter. Aus der Zeitabhängigkeit des Elektrodenpotentials wurden experimentelle Elektrodenkapazitäten berechnet. Man diskutiert den Mechanismus der Wasserstoffelektrode mit Bezug auf

* Manuscript received 1 July 1967.

ein Modell, welches einen schnellen Entladungsschritt für das Wasserstoffion gefolgt von einer Rekombinationsreaktion als geschwindigkeitsbestimmenden Schritt beinhaltet. Das Verhalten der Wasserstoffelektrode an Gold in sauren Sulfatschmelzen ist ähnlich demjenigen dieser Elektrode in wässrigen Lösungen bei Normaltemperatur.

INTRODUCTION

THE KINETICS of hydrogen evolution on gold electrodes has been investigated under different experimental conditions in aqueous solutions by a number of researchers. A comprehensive survey of the results, and a contribution to the hydrogen-electrode reaction on gold as to its dependence on electrode pretreatment and on the nature of the electrolyte dissolved in water, have been published recently.[1,2] These results, involving Tafel slopes which apparently depend on the electrode pre-history, cover the whole range from $2RT/F$ to $RT/2F$ and the apparent exchange cds, determined from extrapolated Tafel lines or low overvoltage data,[3,4] are between $10^{-3.15}$ and $10^{-7.04}$ A/cm^2. Consequently, the various mechanisms already discussed for the hydrogen electrode[5] have been postulated to explain the experimental data, although for several decades the catalytic mechanism has been considered as the most likely reaction path for the hydrogen-electrode reaction on gold.[6–8]

In spite of the numerous studies reported on the hydrogen evolution on gold in aqueous solutions, the literature on this reaction in molten acid salts is very scarce. Data have been published particularly for potassium acid sulphate,[9] and there a linear Tafel plot has been obtained with a slope close to $RT/2F$, which has been mechanistically interpreted in terms of the discharge of a hydrogen ion followed by combination of the hydrogen atoms as the rate-determining step.

A study of the kinetics of the electrochemical formation of hydrogen in the electrolysis of molten potassium acid sulphate on platinum electrodes was made[10,11] and the investigation was then extended to gold electrodes, to correlate the information with that above mentioned for the aqueous systems, in the same way as has been reported previously for platinum electrodes.

Preliminary studies on the effect of the electrode material on the kinetics of the hydrogen-evolution reaction in acid melts[12] have shown that current/voltage curves, plotted according to the Tafel equation, have a wide range of slopes from $RT/2F$ up to about $2RT/F$, depending on the kind of gold electrodes employed, whether these were bright gold, or gold-plated electrodes. These results resemble in some ways those obtained for the aqueous systems.

As part of a systematic investigation on the electrochemical formation of hydrogen in the electrolysis of molten acid sulphates, the kinetics of the reaction was re-investigated under more carefully controlled conditions, over a wide range of temperature and on different prepared gold electrodes. At the same time it was attempted to get some results about the hydrogen-dissolution process in the melt with the same electrodes, the information obtained from both the cathodic and anodic processes being of importance for establishing with more certainty the reaction mechanism.

EXPERIMENTAL TECHNIQUE

The electrolysis cell containing about 600 cm^3 of molten salt was similar to that referred to earlier.[11]

Different kinds of working electrodes were used: (i) bright gold electrodes were made with gold wire (fine gold) of 0·25 mm diameter. These were polished with

alumina–alcohol, degreased and cleaned before each experiment; (ii) gold electrodes prepared by electrodepositing gold on a bright gold base for the purpose, a solution of the complex auric chloride was used;[13] (iii) gold electrodes prepared as indicated in (ii) but on a bright platinum base. The electrodes were used as cathodes in the acid melts for about 30 min at a current of about 50 mA before being employed as working electrodes, either as cathode or anode. Electrodes (ii) and (iii) presented a matt uniform surface. Freshly prepared electrodes were used in each experiment.

The counter-electrode on which either oxygen or hydrogen evolution took place according to the experiment performed, was a platinum wire lodged in a special cell compartment, avoiding any gas diffusion to the working electrode section.

The reference electrode was a platinized platinum wire dipped into the melt, continuously saturated with hydrogen gas, and placed into a Luggin–Haber capillary tip arrangement with a very small pseudo-ohmic drop.

Electrical contacts were made either with gold or platinum wires to the rest of the circuit, avoiding any metal junction within the electrolysis cell. Each section of the cell was kept under a controlled atmosphere. Initially the whole electrolysis cell was kept under nitrogen; later, during the experiments whe whole system was continuously stirred and saturated with purified hydrogen at atmospheric pressure.

Two different electrolytes were used: (i) molten potassium acid sulphate (ii) the eutectic formed by 53·5 mole-% of sodium acid sulphate and 46·5 mole-% of potassium acid sulphate, which has a melting point of 125°C.[14] These two melts covered a temperature range from 182 to 344°C. Experiments were not carried on at lower temperatures because of the high apparent viscosity of the eutectic.[15]

Electrolytes were prepared from Mallinckrodt A. R. chemicals. The salt was first dehydrated in a vacuum system for several days at a pressure lower than 10^{-2} torr. Later it was placed in the cell at the temperature of the experiment for about two days and finally pre-electrolysed for several hours at different cds.[16]

Temperature was read with a Ni–Cr/Ni–Al thermocouple with the hot junction in a glass sheath dipped into the melt close to the working electrode section.

Polarization curves were determined both galvanostatically and potentiostatically. A high impedance potentiostat with a voltage control better than 1 mV was used. The rest of the electrical circuitry was as described before.[17] The range of current densities was from a few $\mu A/cm^2$ to about 10^5 $\mu A/cm^2$.

The build-up of potential of the working electrode during galvanostatic polarization was recorded by photographing the curves from the oscilloscope screen. Decay of potential, at current cessation, was also recorded conventionally. Records of decay and build-up curves ranging from 100 μs to about 10 min covered an interval more than sufficient to establish the steady potential, either when the current was switched off or on.

RESULTS

The main product of the cathode reaction is hydrogen, as was the case for the electrolysis of the melt on platinum. At the highest current densities and temperatures employed, the formation of small amounts of sulphur was observed. The sulphur stayed in suspension in the melt, and the amount formed during one experiment was so small that its evaluation by chemical analysis was not reliable. Sulphur formation in the electrolysis of molten potassium acid sulphate at high current density has been reported.[18]

1. *Cathodic current/voltage curves*

Typical cathodic current/voltage curves corrected for pseudo-ohmic drop are shown in Figs. 1 to 6. The pseudo-ohmic resistance was evaluated from the instantaneous jump of potential read on build-up and decay curves, at different current intensities, its value being between 0·1 and 0·5Ω. The correction was significant at current intensities of more than about 5 mA.

The current/voltage curves obtained for each kind of electrode at different temperatures exhibit some general features. At constant temperature even after successive runs, the Tafel plots are reproducible. Furthermore, within experimental error, they are also coincident when obtained either by raising or lowering the current, this

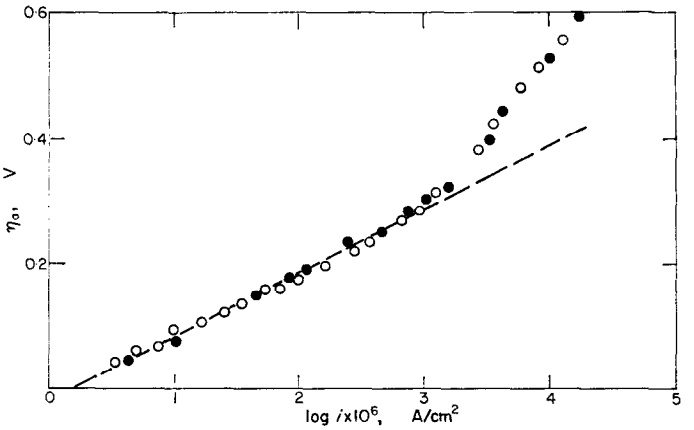

FIG. 1. Cathodic Tafel plot. Bright Au electrodes. T = 182°C. $KHSO_4$-$NaHSO_4$. Galvanostatic run. ●, rising; ○, decreasing.

statement being more strictly correct at the lower cds. No particular distinction can be made between potentiostatic or galvanostatic experiments as far as cathodic current voltage curves is concerned.

The following analysis starts with results obtained on bright gold electrodes, at different temperatures. The cd, i in A/cm^2, is defined in terms of the apparent electrode area, the overvoltage, η in V is the difference between the electrode potential, E_i, at current density i, and the rest potential, E_r, read after current interruption.

At 182°C (Fig. 1) the Tafel plot shows two linear regions: the first, covering a log ($i \times 10^6$) range from 1·0 to 3·0, has a slope, $(b_T)_1$, of 0·102 V. The second linear portion, extending up to log ($i \times 10^6$) = 4·3, has a slope, $(b_T)_2$, of 0·260 V. The transition from the first to the second slope occurs at the overvoltage, η_t, of about 0·300 V.

At 248°C (Fig. 2) the Tafel plot again exhibits two linear portions, the first having a slope of 0·085 V and covering a log ($i \times 10^6$) range from 1·0 to 3·5. At the lowest overvoltages, a clear deviation from this line is now observed. In the range of log ($i \times 10^6$) between 3·6 and about 4·8, a second straight line having a slope of 0·205 V fits the results acceptably although actually the experimental data fit a slight curve. This effect may in part be caused by the increasing rate of bubble formation on the working electrode which changes consequently both the actual electrode area and the pseudo-ohmic drop. This drawback is more notable in the region of highest cd

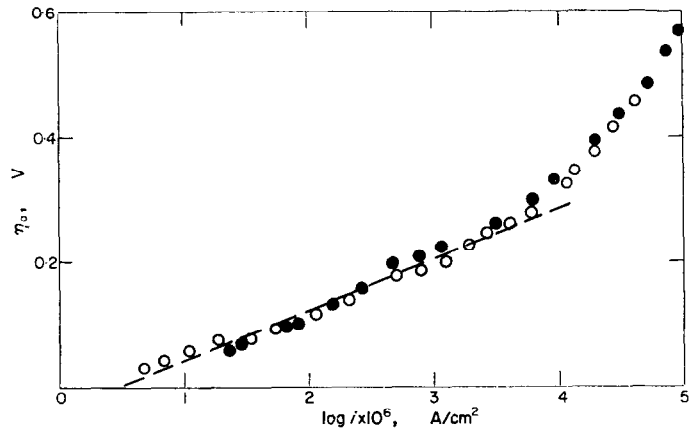

FIG. 2. Cathodic Tafel plot. Bright Au electrodes. T = 248°C. $KHSO_4$-$NaHSO_4$. Galvanostatic run. ●, rising; ○, decreasing.

were both the current and the voltage readings were not stable but exhibited fluctuation. The transition overvoltage at this temperature is about 0·270 V.

At 276°C (Fig. 3) two definite linear regions are again seen in the Tafel plot. A

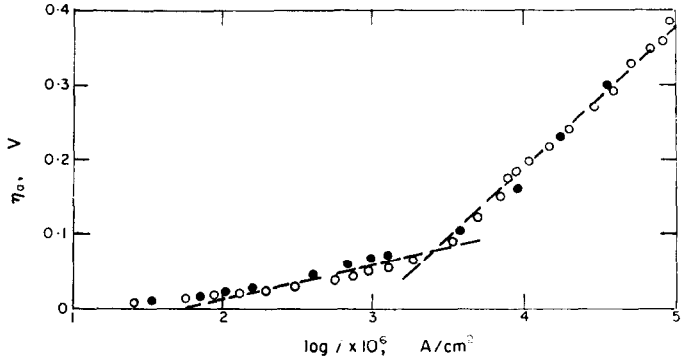

FIG. 3. Cathodic Tafel plot. Bright Au electrodes. T = 276°C. $KHSO_4$. Potentiostatic run. ●, rising; ○, decreasing.

first initial straight line occurs at log ($i \times 10^6$) from 1·7 to 3·2, with a slope of about 0·045 V. The second portion can be fitted with a straight line with a slope of 0·210 V. Beyond log ($i \times 10^6$) = 4·5, the data are not reliable, as already noticed at lower temperatures. The transition from the first to the second straight line occurs at an overvoltage of about 0·070 V.

Data obtained at 344°C are shown in Fig. 4. The plot presents the same features already indicated in Figs. 1–3. For log ($i \times 10^6$) from 2·5 to 4·0, a straight line is observed with a slope of 0·058 V, and beyond 4·0 and up to about 5·0, a second straight line appears with a slope of 0·195 V. The transition region extends from η = 0·070 to about 0·120 V.

Tafel slopes and apparent exchange cds obtained by extrapolation of the corresponding Tafel lines for bright gold electrodes are assembled in Table 1.

Cathodic results obtained with electrodes of the (ii) and (iii) type exhibit a single Tafel line involving a slope higher than that reported for the bright gold electrodes in

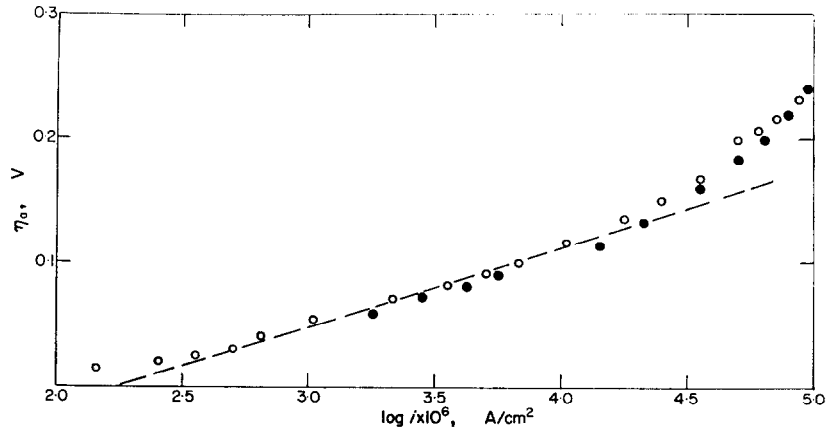

FIG. 4. Cathodic Tafel plot. Bright Au electrodes. T = 344°C. $KHSO_4$. Potentiostatic run. ●, rising; ○, decreasing.

lower cd region. Typical over-voltage/log (current density) plots are shown in Fig. 5 and 6. Tafel parameters deduced from current/voltage curves for those experiments are assembled in Table 2.

2. *Anodic current/voltage curves*

Anodic current/voltage curves were determined at *ca* 270°C with bright gold electrodes, the melt being saturated with purified hydrogen gas. No satisfactory linear Tafel slope was found but there was a net tendency to a limiting current density of 35 μA/cm^2 at 267°C, as shown in Fig. 7. This is also shown in the overvoltage/current density plot of Fig. 8, which shows the linear η/i relationship occurring at overvoltages lower than 2·3(RT/F) V. Taking into account that under these circumstances the rate of the cathodic reaction is not negligible as compared to the rate of

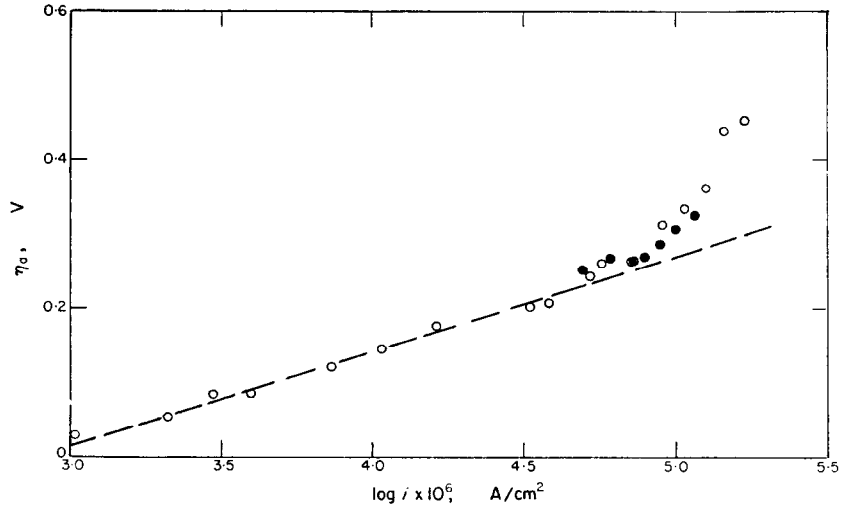

FIG. 5. Cathodic Tafel plot. Au-plated electrode (Au). T = 274°C. $KHSO_4$. Galvanostatic run.

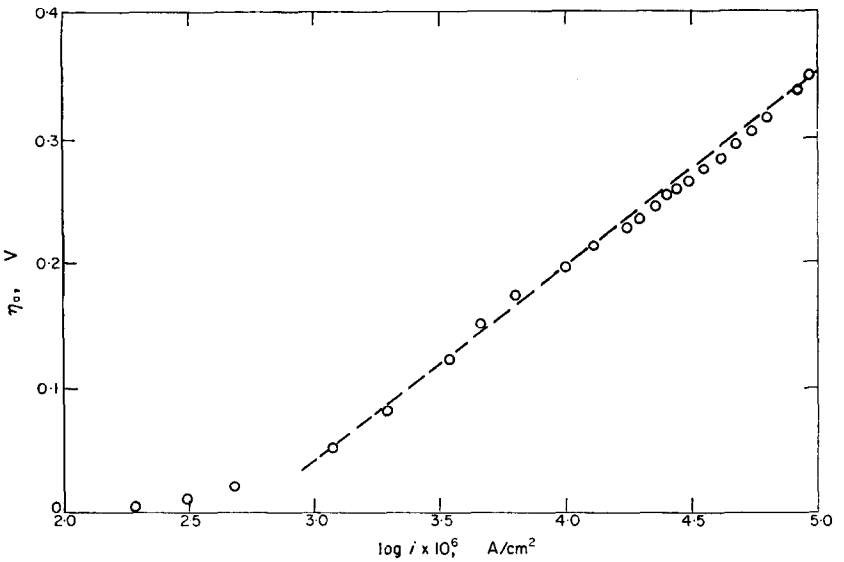

FIG. 6. Cathodic Tafel plot. Au-plated electrode (Pt). T = 270°C. $KHSO_4$. Galvanostatic run.

the anodic reaction, the result is reasonable and allows the estimation of the reaction resistance, R_r, from the initial linear portion. These values are assembled in Table 3.

3. *Decay of cathodic overvoltage*

Experiments on bright gold electrodes will be first considered. Typical decay curves in semilogarithmic plot appear in Figs. 9–14 for different initial current intensities and temperatures.

The simplest relationship between overvoltage and time results from the experiments performed at intermediate temperatures. Thus, at 250 and 280°C (Figs. 10 and 11), the plots show a linear region extending from $\log t = -4$ to $\log t = 0$, where t is the time in seconds elapsed after electrolysis interruption. Data from decay curves are assembled in Table 4. The decay slope, b_d, is equal to $-(\partial\eta/\partial \log t)$. The values of $\log t'$ are obtained by extrapolating the straight lines up to the initial overvoltages. The experimental electrode capacitances, C, have been calculated from t', according to the already known relationship.[19] The decay slope is close to $2{\cdot}3RT/2F$, equivalent to the Tafel slope observed at low cds.

At the lower temperatures the semilogarithmic decay plot (Fig. 9) is characterized by three regions. At the higher and lower overvoltages, the data can be fitted to a straight line whose slope is also close to $2{\cdot}3RT/2F$, as in the region of intermediate temperatures just described. The slopes of those regions are indicated in Table 4. A middle section however exists with a relatively larger slope, and the overvoltage region related to it is close to the corresponding transition overvoltage observed in the overvoltage/log (cd) plot.

At temperatures higher than 300°C, as shown in Fig. 12, no simple relationship between overvoltage and log t is obtained. A decay slope corresponding to a portion of the semilogarithmic plot extending for log t beyond -1 has been tentatively calculated and has been included in Table 4. In this case, the shape of the initial part

Table 1. Kinetic parameters from cathodic current/voltage curves—bright Au electrodes. Average of four runs at each temperature

Temp °C	b_{T_1} V	b_{T_2} V	2·3 (RT/F) V	η_t V	log $(i_0 \times 10^6)_1$	log $(i_0 \times 10^6)_2$	Electrolyte melt
182	0·102 ± 0·005	0·260 ± 0·010	0·090	0·300 ± 0·050	0·23 ± 0·17	1·93 ± 0·17	$KHSO_4$·$NaHSO_4$
248	0·085 ± 0·005	0·205 ± 0·010	0·103	0·270 ± 0·050	0·60 ± 0·20	2·55 ± 0·20	$KHSO_4$·$NaHSO_4$
276	0·045 ± 0·010	0·210 ± 0·010	0·109	0·070 ± 0·050	1·56 ± 0·30	3·10 ± 0·30	$KHSO_4$
344	0·058 ± 0·005	0·194 ± 0·010	0·122	0·120 ± 0·050	2·12 ± 0·40	3·74 ± 0·40	$KHSO_4$

TABLE 2. KINETIC PARAMETERS FROM CATHODIC CURRENT/VOLTAGE CURVES—AU-PLATED ELECTRODES

Temp °C	b_T V	log ($i_0 \times 10^6$)	Range of η V	Electrode	Electrolyte melt
274	0·130 ± 0·010	3·0 ± 0·5	0·05–0·30	ii	$KHSO_4$
274	0·160 ± 0·010	3·0 ± 0·5	0·05–0·30	ii	$KHSO_4$
272	0·144 ± 0·010	2·7 ± 0·2	0·05–0·35	iii	$KHSO_4$
272	0·148 ± 0·010	2·6 ± 0·2	0·05–0·25	iii	$KHSO_4$
275	0·170 ± 0·010	2·8 ± 0·2	0·05–0·30	iii	$KHSO_4$

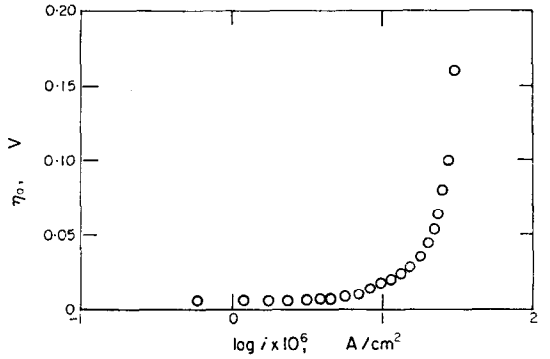

FIG. 7. Anodic Tafel plot. Bright Au electrode. T = 264°C. $KHSO_4$. Galvanostatic run.

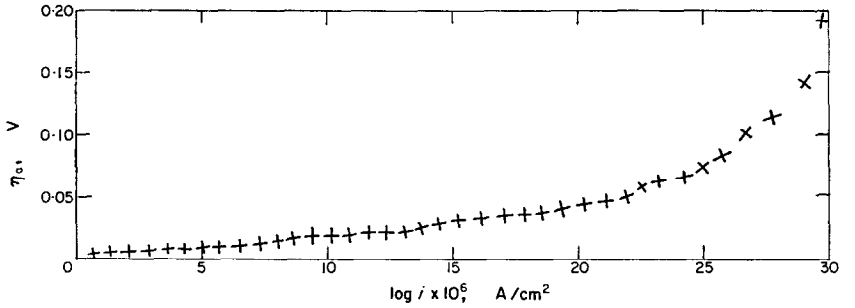

FIG. 8. Low overvoltage polarization. Bright Au electrode. T = 264°C. $KHSO_4$. Anodic run.

TABLE 3. ANODIC REACTION RESISTANCE AND STOICHIOMETRIC NUMBER

Temp °C	$R_r \times 10^{-3}$ V cm^2/A	ν
267	0·9	0·95 ± 0·15
267	1·2	1·26 ± 0·15
264	1·1	1·15 ± 0·15
264	1·0	1·05 ± 0·15

Values calculated with $i_0 = 2{\cdot}5 \times 10^{-6}$ A/cm^2

of the decay curve does not allow the evaluation of the experimental capacitance as already mentioned. Besides, the decay slope appears to depend on the initial electrode potential.

When electrodes of the type (ii) and (iii) are used, the decay of potential occurs logarithmically with time as shown in Figs. 13 and 14, but the decay slope depends

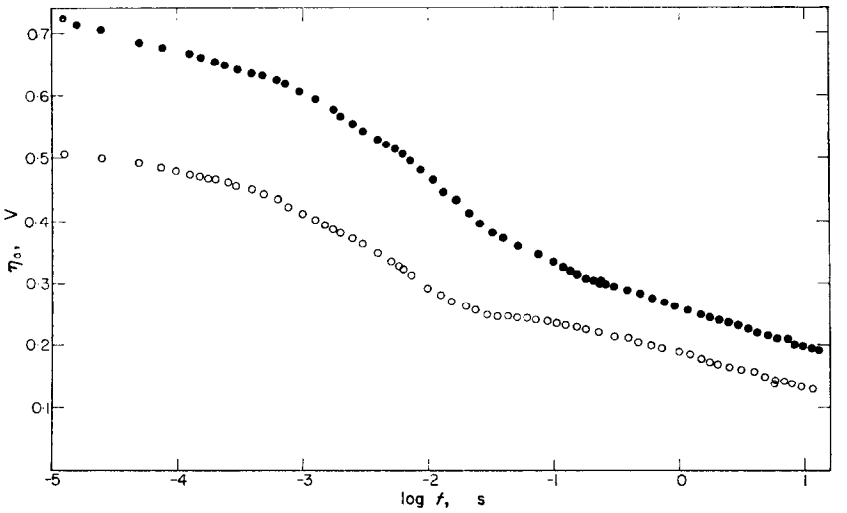

FIG. 9. Semilogarithmic plot of cathodic overvoltage decay. Bright Au electrodes.
T = 182°C. $KHSO_4$-$NaHSO_4$.
○, 8·3 mA/cm²; ●, 92·5 mA/cm².

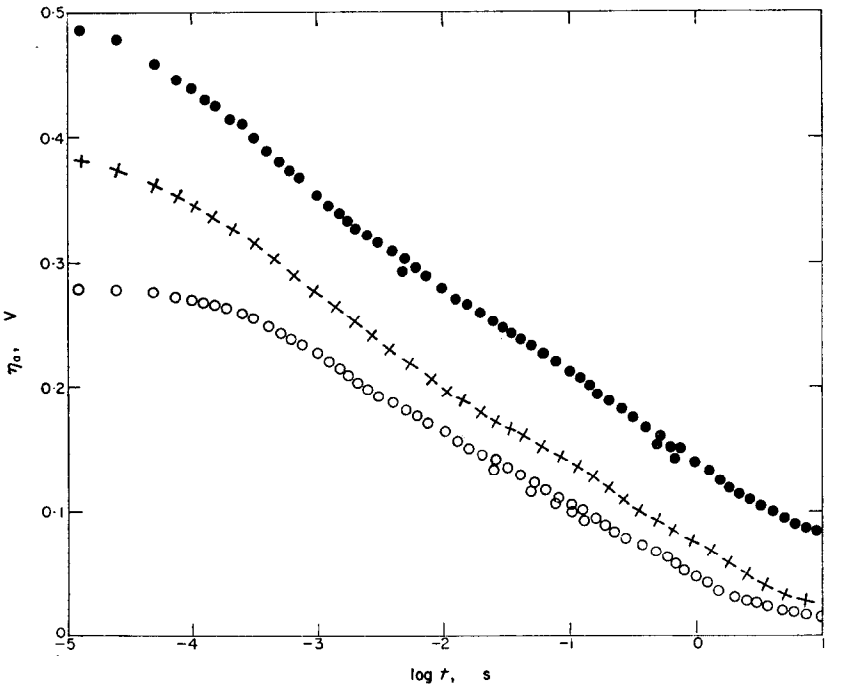

FIG. 10. Semilogarithmic plot of cathodic overvoltage decay. Bright Au electrodes.
T = 248°C. $KHSO_4$-$NaHSO_4$.
○, 3·4 mA/cm²; ×, 19·9 mA/cm²; ●, 57·5 mA/cm².

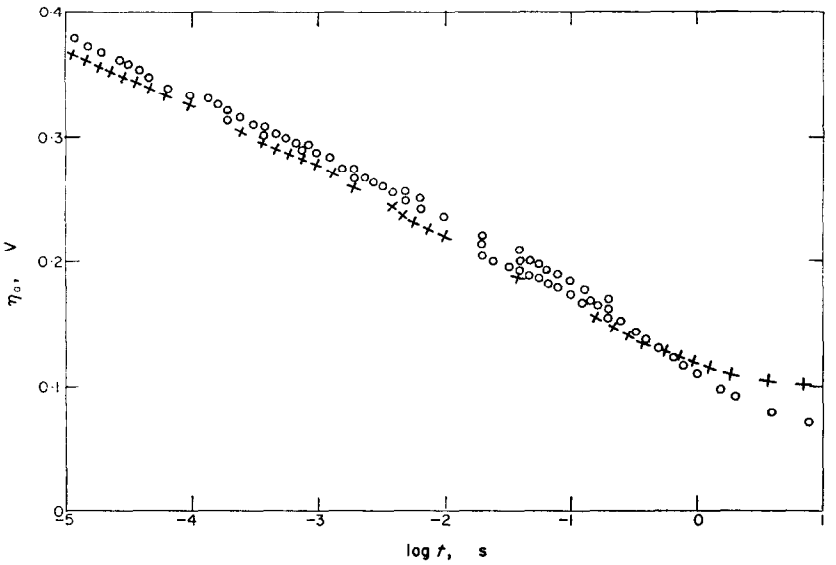

FIG. 11. Semilogarithmic plot of cathodic overvoltage decay. Bright Au electrodes.
T = 280°C. $KHSO_4$.
×, 21·6 mA/cm²; ○, 54·0 mA/cm².

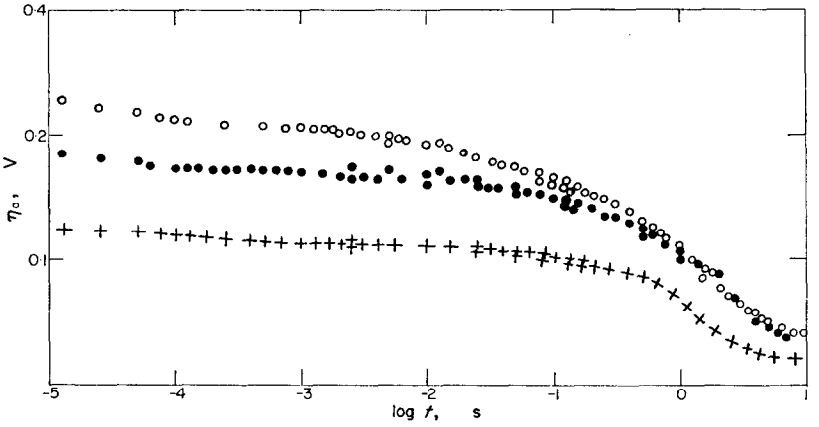

FIG. 12. Semilogarithmic plot of cathodic overvoltage decay. Bright Au electrodes.
T = 344°C. $KHSO_4$.
+, 11·0 mA/cm²; ●, 35·0 mA/cm²; ○, 64·0 mA/cm².

again on the initial electrode potential. The decay slopes, also shown in Table 4, are lower than $2{\cdot}3RT/2F$, approaching this at higher cds. The experimental electrode capacitance is greatly increased as compared to that found for bright gold electrodes, probably due to a significant electrode roughness, which is common for both kinds of electrodes.

4. *Cathodic potential build-up on bright gold electrodes*

The build-up of electrode potential depends on cd and temperature. For cds in the range, 0·01–0·03 A/cm², at 196°C, the electrode reaches about 90 per cent of the final potential value in about 10^{-4} s, while at 333°C, the same percentage is obtained in about 10^{-3} s, as shown in Fig. 15.

TABLE 4. PARAMETERS DEDUCED FROM DECAY CURVES

i A/cm²	η V	b_d V	log t'	C μF/cm²
		182°C—bright Au electrodes.		
0·028	0·625	0·075 ± 0·005	−4·70	19 ± 7
0·058	0·635	0·070 ± 0·010	−4·90	24 ± 7
0·093	0·725	0·075 ± 0·005	−6·00	31 ± 7
		196°C—bright Au electrodes.		
0·009	0·390	0·070 ± 0·010	−4·00	29 ± 7
0·026	0·510	0·078 ± 0·010	−5·10	10 ± 5
0·052	0·640	0·078 ± 0·010	−5·20	10 ± 5
		250°C—bright Au electrodes.		
0·020	0·390	0·066 ± 0·005	−4·70	14 ± 5
0·040	0·458	0·068 ± 0·005	−4·95	15 ± 5
0·064	0·525	0·071 ± 0·005	−4·92	25 ± 5
		265°C—Au-plated electrodes (ii).		
0·034	0·144	0·014 ± 0·003	—	—
0·072	0·260	0·037 ± 0·005	—	—
0·143	0·480	0·053 ± 0·005	—	—
		265°C—Au-plated electrodes (iii).		
0·025	0·280	0·040 ± 0·005	−3·00	1450 ± 300
0·048	0·345	0·055 ± 0·005	−3·10	1600 ± 300
0·064	0·368	0·054 ± 0·005	−3·21	1700 ± 300
		280°C—bright Au electrodes.		
0·022	0·320	0·052 ± 0·005	−4·54	29 ± 5
0·054	0·340	0·057 ± 0·005	−4·90	28 ± 5
0·097	0·400	0·060 ± 0·005	−5·10	26 ± 5
		344°C—bright Au electrodes.		
0·015	0·126	0·030 ± 0·010	—	—
0·050	0·170	0·048 ± 0·010	—	—
0·064	0·215	0·063 ± 0·010	—	—

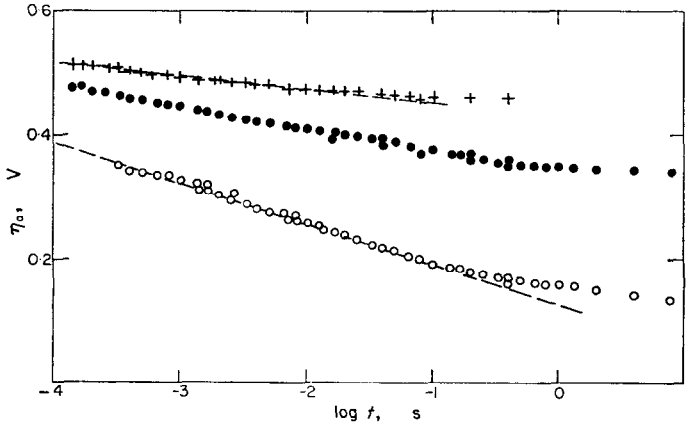

FIG. 13. Semilogarithmic plot of cathodic overvoltage decay. Au-plated electrode T = 270°C. $KHSO_4$.
+, 34·0 mA/cm²; ●, 71·0 mA/cm²; ○, 143 mA/cm².

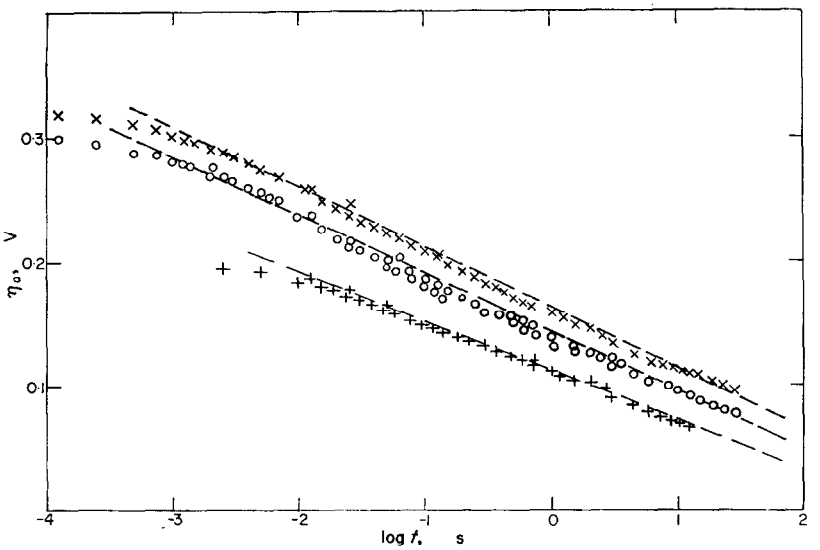

FIG. 14. Semilogarithmic plot of cathodic overvoltage decay. Au-plated electrode (Pt). T = 265°C. $KHSO_4$.
+, 24·8 mA/cm²; ×, 64·0 mA/cm²; ○, 48·2 mA/cm².

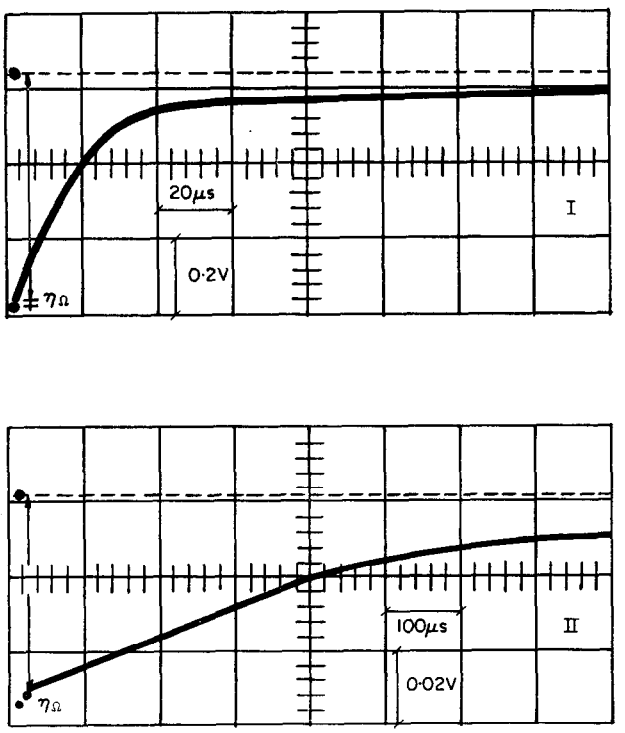

FIG. 15. Cathodic build-up curves.
I. Bright gold electrode, 196°C, $KHSO_4$.$NaHSO_4$; $(I)_{initial}$, 30 mA.
II. Bright gold electrode, 333°C, $KHSO_4$; $(I)_{initial}$, 15 mA.

The build-up curves comprise the initial pseudo-ohmic drop and an initial quasi-linear variation of potential with time. The apparent electrode capacitance at the initial potential was obtained from the initial slope; the results are presented in Table 5. Capacitances are within the same order of magnitude as those reported above from

TABLE 5. DATA FROM CATHODIC BUILD-UP CURVES ON BRIGHT Au ELECTRODES

Temp °C	i A/cm²	C μF/cm²
196	0·044	2·3 ± 0·5
248	0·040	33 ± 5
276	0·065	22 ± 5
330	0·036	21 ± 5

decay curves. However, the results obtained from build-up curves at the lowest temperature are significantly smaller than the average values resulting from decay curves. The opposite effect is noticed in the higher temperature data.

5. The rest potential

The residual potentials were very reproducible and presented a reversible behaviour when either positive or negative current pulses of short duration were applied to the working electrode. Residual potentials are assembled in Table 6.

TABLE 6. REST POTENTIALS
Reference: Pt(H_2, 1 atm)/ acid sulphate melt

Temp °C	E_r V
182	−0·244
198	−0·185
248	−0·140
276	−0·035
333	0·168
344	0·250

The time required for the establishment of the stable residual potential measured against the hydrogen electrode in the melt depended largely on the temperature and on the current intensity at interruption. Thus, at 182°C, decay curves approached a value of about −0·300 V after about 10 s, but after 10 min the final stable potential was −0·244 V. On the other hand, a 344°C, the final value was reached in about 50 s. In general, the higher the current intensity the sooner the final potential was reached.

A monotonous relationship between rest potential and temperature was found; the potential became more positive as temperature increased. It should be noted that at about 280°C, the rest potential changed from negative to positive with respect to the hydrogen electrode.

6. Temperature effect on current/voltage curves

In the circumstances described, the temperature effect on the current/voltage curves can be evaluated either at different fixed overvoltages or at nil overvoltage. The latter procedure was followed by establishing the dependence of the exchange cd on temperature, particularly with the exchange cd extrapolated from the first Tafel

line, which is reliable enough. From the data in Table 1, an Arrhenius plot was drawn, leading to an experimental activation energy, ΔE_a, of 22 ± 4 Kcal/mole. The temperature dependence of the exchange cd derived from the second Tafel line yields the same activation energy, within experimental errors.

DISCUSSION

1. *Preliminary considerations*

In order to present the various possible mechanisms related to the hydrogen electrode on gold in acid sulphate melts, the entity participating in the initial discharge process should be considered. On the basis of electrical conductivity and viscosity studies of low melting acid sulphates,[20] it may be concluded that the acid sulphates are non-associated melts, as far as the electrical conductivity is concerned. The conductivity of these acid salts in the solid and in the ionic melts is largely due to the migration of protons. The structure of potassium bisulphate involves a framework of hydrogen bonds.[21] On the other hand, the thermal decomposition of the alkaline acid sulphates takes place according to

$$2MHSO_4 = M_2S_2O_7 + H_2O, \tag{1}$$

and for M = potassium, the initial rate is 2×10^{-4} mole per mole salt per cm^2 of surface per min, at 220°C.[20] The water formed participates either in metal-ion hydration or reacting with acid sulphate ions according to[22]

$$H_2O + HSO_4^- = H_3O^+ + SO_4^{2-}. \tag{2}$$

These considerations give support to the interpretation of the hydrogen electrode in acid melts formally in the same way already known for aqueous acid solutions.[5]

The experimental results show clearly that the kinetics of hydrogen evolution on gold electrodes in the acid sulphate melts is strongly dependent on the preparation of the electrodes and on the temperature. On bright gold surfaces previously electrolytically reduced with hydrogen two Tafel slopes are observed. At low cd, a limiting value of $RT/2F$ is approached, particularly at intermediate temperatures, while at large cd, a second limiting value of $2RT/F$ appears. Thus, two apparent exchange cds can be defined, related respectively to each Tafel slope. The situation appears, however, more complex in the low temperature region, where the Tafel slopes show a tendency to be near RT/F in the low cd region and to exceed $2RT/F$ in the high cd region. At the highest temperature, on the other hand, there is a tendency of the first Tafel slope to be smaller than $RT/2F$. On gold-plated electrodes, there is a Tafel line only in the whole region of cd investigated, its slope being RT/F thereabouts.

The decay of cathodic overvoltage yields always a decay slope (from overvoltage/log t curves) which is remarkably low. In the simpler cases, that is for bright gold electrodes and the intermediate temperature region, a value of the decay slope close to $RT/2F$ is observed, which is similar to the results obtained from potential decay on gold-plated electrodes at high cds. In other experiments, the decay slope is usually lower than $RT/2F$, and at the lowest temperatures as well as at the highest ones, there is an interval where the decay curves exhibit a rather peculiar behaviour, as already mentioned in detail.

Finally, the electrode experimental capacitances obtained either from decay or

build-up curves are relatively low, and it is very difficult to decide about any dependence on electrode potential. In the case of gold-plated electrodes, the larger experimental capacitance should be in principle related to the actual increase of electrode area. From the results, a factor about 50 must be assigned to the electrode roughness.

2. Probable reaction mechanism related to the hydrogen electrode on gold in acid sulphate melts

The simple kinetic treatment of the hydrogen electrode reaction on gold can proceed on the assumptions that Langmuir adsorption isotherm conditions prevail on the electrode as far as the intermediate reaction products is concerned, and that no appreciable ionic adsorption occurs.

The mechanisms derived from these assumptions proved useful to interpret the same reaction on platinum electrodes where they appeared formally analogous to those derived for aqueous solutions.[11,12] Consequently, the reaction starts with the discharge of a hydrogen ion in the double layer; the latter, in the absence of water, may be considered as a bare ion partially linked to acid sulphate ions by hydrogen bonding. Taking into account the previous cathodic treatment of the gold electrodes, is also reasonable to assume that the discharge occurs on an oxide-free gold, as follows,

$$(H^+)_{d1} + Au + e = Au(H). \tag{3a}$$

The fate of the hydrogen atoms formed on the gold surface is mainly related to molecular hydrogen formation, by the two following known steps,

$$Au(H) + Au(H) = H_2 + 2Au \tag{3b}$$

or

$$Au(H) + (H^+)_{d1} + e = H_2 + Au. \tag{3c}$$

The three main reaction mechanisms, which include reactions (3a), (3b) and (3c) are: Mechanism (i), reaction (3a) is the rate-determining step. Mechanism (ii), reaction (3a) is followed by reaction (3b) as the rate-determining step. Mechanism (iii), reaction (3a) is followed by reaction (3c) as the rate-determining step. Under these circumstances each mechanism is characterized by a definite Tafel slope.[5]

If the degree of coverage by hydrogen atoms is intermediate, say between 0·2 and 0·8, then the Langmuir conditions are in principle no longer valid, and a dependence of the standard free energy for the adsorption of the intermediate species on the degree of coverage should be considered as consequently affecting the rate equations. The theoretical rate equations derived for this situation have been already considered for the different possible mechanisms of reaction related to the hydrogen evolution in aqueous systems.[23,24] The characteristics of mechanisms (i) to (iii) have been deduced by various authors[5,25] and are summarized in the recent literature.[26] The conclusion drawn for this case is that the unambiguous elucidation of the reaction mechanism by an analysis purely based on the Tafel slopes is not feasible.

Assuming however that the transfer coefficient assisting the cathodic process is 0·5, the slope $RT/2F$ can be related to a mechanism involving the discharge and combination reactions where the latter is the rate-determining step, and the standard free energy of adsorption is $\Delta G^\circ \gg 0$, and consequently, the degree of coverage at equilibrium approaches zero. The slope RT/F, which in the case of gold-plated electrodes is definitely established, may be related to a surface of greater activity, which comprises

a relatively lower standard free energy of adsorption, $\Delta G^\circ \approx 0$, and, therefore, a degree of coverage at equilibrium which may be between 0·2 and 0·8. This must be also related to a probable decrease of ΔG° for gold-plated electrodes and an increase of the number of active sites on the electrode surface. The situation may in principle be the same for bright gold electrodes, probably due, at least in part, to an activation of the surface by hydrogen atoms at high cd.

Nevertheless, at least three drawbacks in the interpretation of the results in the high overvoltage region should be taken into account, namely, (i) the fact that bubbles are formed and act by blocking locally the electrode surface. This effect should be more significant at lower temperatures, when the viscosity of the melts is appreciably high. (ii) At the highest overvoltages, the hydrogen atoms produced at a higher rate, yield a higher steady concentration on the electrode surface, this favouring at least two types of processes, the reduction of species present in the molten salt and the penetration of hydrogen in the metal. The former is related to sulphur formation. This, occurring on the electrode, may also contribute to change its actual surface. This difficulty may be of greater importance at the higher temperatures where sulphur formation appears to be more favoured. The penetration of hydrogen in the metal is evidenced through the form of overvoltage decay immediately after current interruption, as is discussed further on. (iii) The existence of an overvoltage contribution related to the diffusion of molecular hydrogen out of the working electrode region. This also must be particularly considered at low temperatures where some peculiar effects are observed in the current/voltage curves as well as in the decay curves. Finally, within these difficulties, it should also be pointed out that in the range of highest temperatures, the region related to the first Tafel line involves relatively low overvoltages. Consequently, although results on bright gold at high cds fit well into the mechanistic picture above described, they should be regarded with caution because of the various processes previously annotated.

Therefore, to elucidate the hydrogen electrode reaction mechanism besides the Tafel slopes and exchange cd, the stoichiometric number should also be considered, as well as the current/overvoltage characteristic of the anodic process and the experimental activation energy. The stoichiometric number can be estimated from the anodic current/voltage curves at low overvoltages. The reaction resistance obtained from the anodic curves, when $\eta \to 0$, is related to the stoichiometric number, ν, according to

$$\nu = \frac{nFi_0}{RT}\left(\frac{\partial \eta}{\partial i_a}\right)_{\eta \to 0}, \tag{4}$$

where n is the total number of electrons entering the reaction and i_0 the apparent exchange cd which resulted from the extrapolation of the lower cathodic Tafel line. Values of ν calculated from (4) are assembled in Table 3. From these data it is concluded that the stoichiometric number is very likely one. This finding yields thus a further support to the combination reaction as the rate-determining step. Naturally, another argument in favour of it must still be added, since a value of $\nu = 1$ appears also to be related to the ion-plus-atom reaction as the rate-determining step, although in the latter case under no circumstances will a slope of $RT/2F$ be found.

However, the characteristics of the hydrogen-electrode reaction comprising the combination of hydrogen atoms on the electrode surface as the rate-determining step,

implies that the anodic Tafel slope approaches infinity, as the anodic current density, i_a, approaches i_0, and the latter should be equal to the experimental limiting cd, i_L, of the anodic reaction. This result has actually been observed, as shown in Fig. 7, but it by itself is however not sufficient. Thus, if the anodic hydrogen-dissolution reaction were a convective-diffusion-controlled process, the expected anodic limiting cd, calculated assuming a hydrogen solubility in the melt of the order of 10^{-6} mole/cm^3, would be within the order of magnitude already mentioned for i_0. So this point requires further study with a different experimental approach, but at present it fits within the interpretation advanced for the electrode reaction.

However, in spite of those possible interpretations, the results of the anodic reaction in the melt appear apparently simpler than the anodic dissolution of hydrogen in acid aqueous systems. For the latter, the process is rather more complex because of specific adsorption interferences which reflect in the existence of a maximum in current/voltage curves.[27]

The appearance of various Tafel slopes in the hydrogen discharge process may also be explained on the basis of the dual mechanism, which relates the probable reaction mechanism of the hydrogen electrode with the catalytic activity of the metals.[1,8] This approach yields theoretical Tafel slopes between $RT/2F$ and $2RT/F$ and predicts a region in the overvoltage/log (current) plot where a transition between those slopes occurs. Finally, the main conclusion is that the initial discharge reaction as the rate-controlling step in the reaction scheme should be discarded, and the combination step must be considered as the probable rate-determining step.

3. *The thermal effect on the reaction rate*

From the dependence of the apparent cd densities on temperature for the bright gold electrodes, the experimental activation energy of 22 ± 4 Kcal/mole was obtained. This result is not very different from that reported for the same reaction on bright platinum electrodes,[10] and suggests that in the temperature and intensity range investigated, the mechanism of the electrochemical reaction is probably the same.

Accordingly, taking the experimental activation energy, ΔE_a, as the corresponding change of enthalpy, ΔH_a, the pre-exponential factor, B, of the rate equation is given by

$$\log B = \log i_0 + \frac{\Delta H_a}{2{\cdot}3RT}. \tag{5}$$

At 267°C, taking $\log i_0 = -4{\cdot}9 \pm 0{\cdot}3$, we get $\log B = 4{\cdot}1 \pm 1{\cdot}8$. This figure is near the value of 3 ± 2 found for different hydrogen electrodes in aqueous solutions[28] and lately also obtained for the same reaction in non-aqueous electrolytes.[29] From this figure, which depends principally on the entropy change in the activated process, the *maximum* entropy change, $\Delta S^{\ddagger}$, can be estimated. Thus

$$B = \frac{kT}{h}\,\varepsilon C_i \exp\left(\frac{\Delta S^{\ddagger}}{R}\right), \tag{6}$$

where ε is the unit charge and, C_i is the surface concentration of the reacting species, in this case hydrogen atoms, whose maximum value is about 10^{15} atom/cm^2, assuming

one atom per atom of the ideal metal lattice. Thus, at 519°K, we get

$$B = 1{\cdot}8 \times 10^9 \exp\left(\frac{\Delta S^{\ddagger}}{R}\right). \tag{7}$$

Taking $B = 10^{4{\cdot}1 \pm 1{\cdot}8}$, the entropy change in the activated process can be estimated as $-23{\cdot}5 \pm 4{\cdot}0$ e.u. Assuming the surface concentration is one tenth of the figure used before, the entropy change is $-18{\cdot}9 \pm 4{\cdot}0$ e.u. These values are congruent with the mechanism already discussed, since the passage from two loosely bound hydrogen atoms to the more ordered transition state complex should involve a rather large entropy decrease.

Let us assume that the experimental activation energy is related almost completely to energy changes occurring in the rate-determining step, an approximation which can be justified considering the symmetrical electrode system involving the hydrogen electrode reaction. Then, with the hypothesis that hydrogen atoms are bound to gold comprising just the hydrogen–gold bond energy of the metal hydride, the maximum activation energy expected for the recombination step would be

$$(\Delta E_a)_{max} \approx 2D_{H-Au} - D_{H_2}, \tag{8}$$

neglecting any contribution from the metallic state. Taking for $D_{H_2} = 103{\cdot}2$ Kcal/mole and $D_{H-Au} = 72$ Kcal/mole,[30] we get $(\Delta E_a)_{max} \approx 41$ Kcal/mole. As a matter of fact, the actual value is lower than that approximated with (8). However, this limiting calculation is not entirely satisfactory because the bond energy of hydrogen adatoms should be lower than that of the hydride bond. If ΔH_d represents the initial enthalpy of adsorption, the experimental activation energy can be approximately equated to it through the following expression

$$\Delta E_a \approx \Delta H_d = 2D_{(H)Au} - D_{H_2}. \tag{9}$$

The dissociation energy of the hydrogen adatom, $D_{(H)Au}$, can be calculated from Pauling's equation,[31,32] which involves the metal–metal bond energy, the hydrogen molecule dissociation energy and the electronegativities of the metal and atomic hydrogen.

Application of (9) to the experimental results implies that the binding energy of hydrogen adatoms on gold is 61 ± 4 Kcal/mole, a figure which is slightly higher than the value reported from adsorption of the gas on clean gold surfaces and lower than the corresponding figure for platinum surfaces.[33] This energy difference supposes a preferential adsorption of hydrogen atoms on platinum in the case of using platinum–gold alloy electrodes, as was observed in aqueous media.[34,35] Consequently as the binding energy of hydrogen adatoms is not very different, the kinetic behaviour of the hydrogen electrode on gold and platinum should be more or less the same, as seems to occur also in acid sulphate melts.

4. *The non-steady measurements*

Two results were principally obtained from the non-steady measurements, namely, the decay slope and the apparent electrode capacitance at different electrode potentials. As to the latter, the fact that electrode capacitances for gold-plated electrodes are

higher by a factor of about 50, as compared to bright electrodes, and that the same factor results from the extrapolated apparent exchange cd, as already indicated, that figure should be assigned chiefly to a greater roughness of those electrodes.

Except for these cases, the electrode capacitances are relatively low, and particularly in the range of temperature from 182 to about 300°C they are in the range from 10 to 30 $\mu F/cm^2$ and no definite variation with electrode potential can be established. These results are in agreement with capacitance measurements performed during hydrogen evolution in acid aqueous solutions, where the capacitances are of the order of 10 $\mu F/cm^2$, and no significant variation of capacitance with potential in a range of about 0·5 V was observed.[36]

The decay slopes obtained on bright gold electrodes at intermediate temperatures are very close indeed to $RT/2F$, as is observed in the Tafel line for the lower overvoltage region. Thus, the behaviour of the electrochemical reaction under non-steady conditions yields a further support to the interpretation given at present with a reaction mechanism involving the discharge reaction followed by the combination reaction as the rate-determining step, assuming that the degree of coverage of hydrogen atoms does not depend appreciably on the electrode potential.

The situation seems somewhat complicated at the lower and higher temperatures investigated. In the former region the $RT/2F$ decay slope is observed, but it appears after the overvoltage has reached values corresponding to the first Tafel-line region. This electrode response in the case of decay, as well as the existence of a region of Tafel slope higher than $2RT/F$ in the current/voltage curves, is probably related in part to slower hydrogen gas diffusion due to the high viscosity of the melt at the lower temperatures.

The potential decay at high temperatures exhibits a relatively large region in the semilogarithmic plot where the potential change is small. Decay curves at high temperatures yield values of capacitance that, although somewhat scattered, are larger than those previously annotated at lower temperatures. This effect, however, can be explained if a certain amount of hydrogen is dissolved in the metal. Gold is usually considered a metal "which possesses no occlusive capacity sufficient to be detected by the usual methods."[37,38] However, as already stated for the case of the hydrogen electrode in the aqueous solutions,[39] taking into account the dimensions of the cubic close-packed structure of gold, there seems to be no spatial reason why hydrogen should not dissolve in gold. It may be reasonable to assume that if the diffusion of hydrogen from the bulk of the metal to the electrode surface tends to maintain the surface concentration of hydrogen atoms corresponding to the electrode potential at current interruption, the electrode potential will remain approximately constant. The existence of this effect will depend on the rate of diffusion of hydrogen through the metal and of the rate of the electrochemical reaction. A further discussion of this point based upon these processes will be dealt with in a future publication where the hydrogen-electrode reaction on palladium electrodes and acid sulphate melts is reported.[40] A similar explanation was advanced quite recently for electrode reactions on porous graphite electrodes in nitrite melts.[41]

In the case of gold-plated electrodes a decay slope of $RT/2F$ is approached only at high current densities, being smaller than that in other circumstances. This fact agrees with a higher reactivity of gold-plated electrodes for hydrogen atoms becoming more firmly bound to the electrode surface when an interpretation of the electrochemical

reaction in terms of the combination step already discussed is arrived at. This is in principle similar to that occurring under certain circumstances on platinum electrodes in aqueous solutions.[42] The decay slopes lower than those reported from the steady measurements are explicable by the same reaction mechanism, with an intermediate degree of coverage.[19,43]

From the previous discussion and considering the characteristics of the rest potential of the gold electrode in acid sulphate melts, it is concluded that it behaves as "a non-equilibrium atomic hydrogen electrode," as already found in acid aqueous solutions.[39]

Finally, it may be said that the hydrogen-evolution reaction on gold in acid sulphate melts is not much different from the reaction occurring in aqueous acid media. The reaction mechanism is the discharge of a hydrogen ion followed by the combination of atoms as the rate-determining step. These conclusions fits the mechanistic expectation based on the electronic structure of the metal. The present work encourages a deeper study of the hydrogen-electrode reaction in melts on platinum electrodes.

Acknowledgements—This work was in part done with financial aid from the Consejo Nacional de Investigaciones Cientificas y Técnicas of Argentina. We are indebted to Dr. A. J. Calandra for his participation in the experiments with gold-plated electrodes. F.D.V. thanks the Facultad de Ciencias Fisico matematicas, Universidad de La Plata, for the scholarship granted during the course of the present work.

REFERENCES

1. H. KITA, *J. electrochem. Soc.* **113**, 1095 (1966).
2. G. M. SCHMID, *Electrochim. Acta* **12**, 449 (1967).
3. M. BREITER, H. KAMMERMEIER and C. A. KNORR, *Z. Elektrochem.* **60**, 454 (1956).
4. N. PENTLAND, J. O'M. BOCKRIS and E. SHELDON, *J. electrochem. Soc.* **104**, 182 (1957).
5. K. VETTER, *Elektrochemische Kinetik*, pp. 412–430. Springer, Berlin (1961).
6. J. HORIUTI and T. NAKAMURA, *J. chem. Phys.* **18**, 395 (1950).
7. J. HORIUTI, T. KEII and K. HIROTA, *J. Res. Inst. Catalysis Hokkaido Univ.* **2**, 1 (1951–53).
8. J. HORIUTI, A. MATSUDA, M. ENYO and H. KITA, *Proc. 1st. Australian Conf. Electrochemistry*, p. 750. Pergamon, Oxford (1965).
9. A. M. SHAMS EL DIN, *Electrochim. Acta* **7**, 613 (1962).
10. H. A. VIDELA and A. J. ARVIA, *Electrochim. Acta* **10**, 21 (1965).
11. A. J. ARVIA, A. J. CALANDRA and H. A. VIDELA, *Electrochim. Acta* **10**, 33 (1965).
12. A. J. ARVIA, A. J. CALANDRA and H. A. VIDELA, *Anal. Asoc. Quimica Arg.* **54**, 143 (1966).
13. A. G. GRAY, *Modern Electroplating*, p. 252. Wiley, New York (1953).
14. D. INMAN and N. S. WRENCH, *Brit. Corr. J.* **1**, 246 (1966).
15. A. J. ARVIA, A. J. CALANDRA and H. A. VIDELA, in preparation.
16. F. LEBER, *Rapp. C.E.A.*-R 2567, p. 59. Centre d'Etudes Nucléaires, Saclay (1964).
17. W. E. TRIACA and A. J. ARVIA, *Electrochim. Acta* **10**, 409 (1965).
18. S. TAJIMA, M. SODA, T. MORI and N. BABA, *Electrochim. Acta* **1**, 205 (1959).
19. E. GILEADI and B. E. CONWAY, in *Modern Aspects of Electrochemistry*, ed. J. O'M. Bockris and B. E. Conway, Vol. 3, p. 362. Butterworths, London (1964).
20. S. E. ROGERS and A. R. UBBELOHDE, *Trans. Faraday Soc.* **46**, 1051 (1950).
21. L. H. LOOPSTRA and C. H. MACGILLAVRY, *Acta Crystollogr.* **11**, 349 (1958).
22. F. LEBER, *op cit* p. 8.
23. R. PARSONS, *Trans. Faraday Soc.* **54**, 1053 (1958).
24. R. PARSONS, *J. chim. Phys.* **49**, C-82 (1952).
25. P. D. LUKOVTSEV, *Zh. fiz. Khim.* **21**, 589 (1947).
26. P. DELAHAY, *Double Layer and Electrode Kinetics*, p. 267. Interscience, New York (1965).
27. A. N. FRUMKIN, in *Advances in Electrochemistry and Electrochemical Engineering*, ed. P. Delahay and C. W. Tobias, Vol. 3, p. 287. Interscience, New York (1963).
28. K. L. LAIDLER, S. GLASSTONE and H. EYRING, *J. chem. Phys.* **7**, 1053 (1939).
29. J. HORIUTI and H. KITA, *J. Res. Inst. Catalysis Hokkaido Univ.* **12**, 1 (1964).
30. T. L. COTTRELL, *The Strengths of Chemical Bonds*, p. 274. Butterworths, London (1952).
31. D. D. ELEY, *Discuss. Faraday Soc.* **8**, 34 (1950).
32. L. PAULING, *The Nature of the Chemical Bond.* Cornell University Press, Ithaca, New York (1945).

33. G. EHRLICH, *Ann. N.Y. Acad. Sci.* **101**, 722 (1963).
34. K. A. LAPTEVA, T. I. BORISOVA and M. G. SLINKO, *Zh. fiz. Khim.* **30**, 61 (1956); *C. A.* 9095c (1956).
35. M. W. BREITER, *Trans. Faraday Soc.* **61**, 749 (1965).
36. G. M. SCHMID and N. HACKERMAN, *J. electrochem. Soc.* **109**, 243 (1962).
37. D. P. SMITH, *Hydrogen in Metals*, p. 282. Univ. Chicago Press, Chicago (1948).
38. R. M. BARRER, *Diffusion in and through Solids*, p. 146. Cambridge Univ. Press, London (1951).
39. D. J. G. IVES and S. SWAROOPA, *J. chem. Soc*, 3489 (1955).
40. A. J. ARVIA, A. J. CALANDRA and H. A. VIDELA, in preparation.
41. A. J. ARVIA and A. J. CALANDRA, *Electrochim. Acta* **12**, 1441 (1967).
42. M. BREITER, *Electrochim. Acta* **7**, 601 (1962).
43. B. E. CONWAY and P. L. BOURGAULT, *Trans. Faraday Soc.* **58**, 593 (1962).